ChemPubSoc Europe

DOI: 10.1002/chem.201706162

CHEMISTRY A European Journal Full Paper

Prebiotic Chemistry |*Hot Paper*|

Silica Metal Oxide Vesicles Catalyze Comprehensive Prebiotic Chemistry

Bruno Mattia Bizzarri,[a] Lorenzo Botta,[a] Maritza Iveth Pérez-Valverde,[b] Raffaele Saladino,*[a] Ernesto Di Mauro,[a] and Juan Manuel García-Ruiz*[b]

Abstract: It has recently been demonstrated that mineral self-assembled structures catalyzing prebiotic chemical reactions may form in natural waters derived from serpentinization, a geological process widespread in the early stages of Earth-like planets. We have synthesized self-assembled membranes by mixing microdrops of metal solutions with alkaline silicate solutions in the presence of formamide (NH_2CHO), a single-carbon molecule, at 80 °C. We found that these bilayer membranes, made of amorphous silica and metal oxide/hydroxide nanocrystals, catalyze the condensation of formamide, yielding the four nucleobases of RNA, three amino acids and, several carboxylic acids in a single-pot experiment. Besides manganese, iron and magnesium, two abundant elements in the earliest Earth crust that are key in serpentinization reactions, are enough to produce all these biochemical compounds. These results suggest that the transition from inorganic geochemistry to prebiotic organic chemistry is common on a universal scale and, most probably, occurred earlier than ever thought for our planet.

Introduction

It has long been thought that minerals have a significant catalytic role in the synthesis of life's building blocks.[1–3] Pioneering work successfully demonstrated the formation of amino acids, nucleobases, and other molecular bricks of life from simple organic molecules, with hydrogen cyanide (HCN) being the precursor compound most used in prebiotic chemistry experiments so far.[4–6] Among the alternatives to HCN that meet the prebiotic requirements of stability and reactivity, formamide (NH_2CHO), a single-carbon organic molecule, has been proven to be very successful both in terms of the variety of relevant molecules synthesized and in yield. For instance, formamide has been demonstrated to condense into carboxylic acids, several amino acids, as well as into purines and pyrimidines.[7,8] The condensation reaction is catalyzed by temperature, by several minerals, and by high-energy proton irradiation.[9] Formamide is present in a variety of star-forming environments,[10,11] and it has also been found on several comets of the solar system.[12,13] In fact, formamide appears to be a critical intermediary in Miller-type reactions.[14]

No matter the route, whether HCN or NH_2CHO, in addition to minerals, the geological niche(s) for prebiotic chemistry needs to be fed with molecular hydrogen, carbon, and nitrogen, within a reduced or anoxic environment where the formation of stable organic molecules can thrive towards complexity. The most efficient reaction providing these molecular compounds and the proper physicochemical environment is the interaction of water with olivine minerals, the so-called serpentinization reaction.[15,16] Serpentinization, along with the Sabatier reaction and Fischer–Tropsch-type reactions, is the most productive chemical scenario for the synthesis of organic molecules. It is a scenario in which mineral/organic chemistry works today in a few specific geological sites but it is thought to have been working on a global scale during the early Earth at Hadean times. It is also a scenario where that singular chemistry plays and has been playing beyond the Earth, at least in Earth-like planets, moons, and interstellar dust, where formamide is fully available. Interestingly, serpentinization environments may form alkaline waters rich in silica. It has been experimentally demonstrated that these alkaline waters induce the growth of self-assembled mineral structures,[17] including silica/carbonate biomorphs mimicking the morphology of primitive organisms, calcium carbonate mesocrystals similar to those formed in biominerals, and silica metal oxy/hydroxide bilayer membranes, also known as silica gardens, with interesting catalytic properties.[18–20] We have synthesized these mineral membranes in alkaline silica-rich solutions similar to those deriving from serpentinization reactions in the presence of formamide at 80 °C. Rather than pellets of salts used in classical silica garden experiments, we used microdrops of solutions of different soluble metal salts, thus mimicking a more realistic geochemical environment. We show that the four nucleobases

[a] *Dr. B. Mattia Bizzarri, Dr. L. Botta, Dr. R. Saladino, Dr. E. Di Mauro*
Ecological and Biological Sciences Department (DEB)
University of Tuscia, Via S. Camillo de Lellis snc, 01100, Viterbo (Italy)
E-mail: saladino@unitus.it

[b] *Dr. M. I. Pérez-Valverde, Dr. J. M. García-Ruiz*
Laboratorio de Estudios Cristalográficos, Instituto Andaluz de Ciencias de la Tierra, Consejo Superior de Investigaciones Científicas-Universidad de Granada, Avenida de las Palmeras 4, Armilla, Granada 18100 (Spain)
E-mail: juanma.garciaruiz@gmail.com

Supporting information and the ORCID number for the author of this article can be found under https://doi.org/10.1002/chem.201706162.

of RNA, three amino acids, and several carboxylic acids relevant to key metabolic cycles, can be obtained in a robust and simple one-pot reaction even in the absence of radiation.

Results and Discussion

The experiments to explore the formation of membranes by using microdrops were performed with solutions of $FeCl_2$, $FeCl_3$, and $MnCl_2$. The formation of membranes was observed at pH as low as 10.4 and silica concentration of 0.75 mol L^{-1} (Figure 1 A). Upon mixing the microdrops of the salt solution with the silicate solution, a metal–silica membrane is formed surrounding the drop. The initial microdrops expand as a result of osmotic forces until reaching a critical size beyond which they break, releasing the inner metal-rich acidic content into the alkaline silicate solution (Figure 1 B, and Video S1 in the Supporting Information). The jet of solution arising from the breaking point creates a new tubular structure that grows into the silicate solution, eventually breaking and forming new tubular membranes. The complexity of the tubular structure and the degree of breaking depends on the concentration and viscosity of the salt and silicate solutions. The lower the pH and the silica concentration, the larger the degree of disruption of the membrane. This behavior, which was observed for all the tested salts, ensures that formamide, initially located in the alkaline silica solution, enters also into contact with the metal-rich solution during the formation of the silica/metal membrane. This allows the catalysis of the condensation of formamide by the inner side of the membrane, made of metal oxide/hydroxide nanoparticles, and by the outer part of the membrane made of porous silica.[21,22] The growth of the structures is visible for several minutes but the chemical reaction is known to last for several hours.[18] Therefore, unlike previous experiments in which passive membranes were used, the condensation of formamide occurs while the reaction leading to the formation of the membranes is active.

Accordingly, to optimize the catalysis in the formamide experiments, we selected a low silica concentration (1.65 mol L^{-1}) and pH (11.5). The condensation experiments were performed by pouring drops of the saturated solutions of the appropriate metal salt [$ZnCl_2$, $FeCl_2{\cdot}4H_2O$, $CuCl_2{\cdot}2H_2O$, $MnCl_2$, $Fe_2(SO_4)_3{\cdot}9H_2O$, $Cu(NO_3)_2$, and $MgSO_4$] to sodium silicate con-

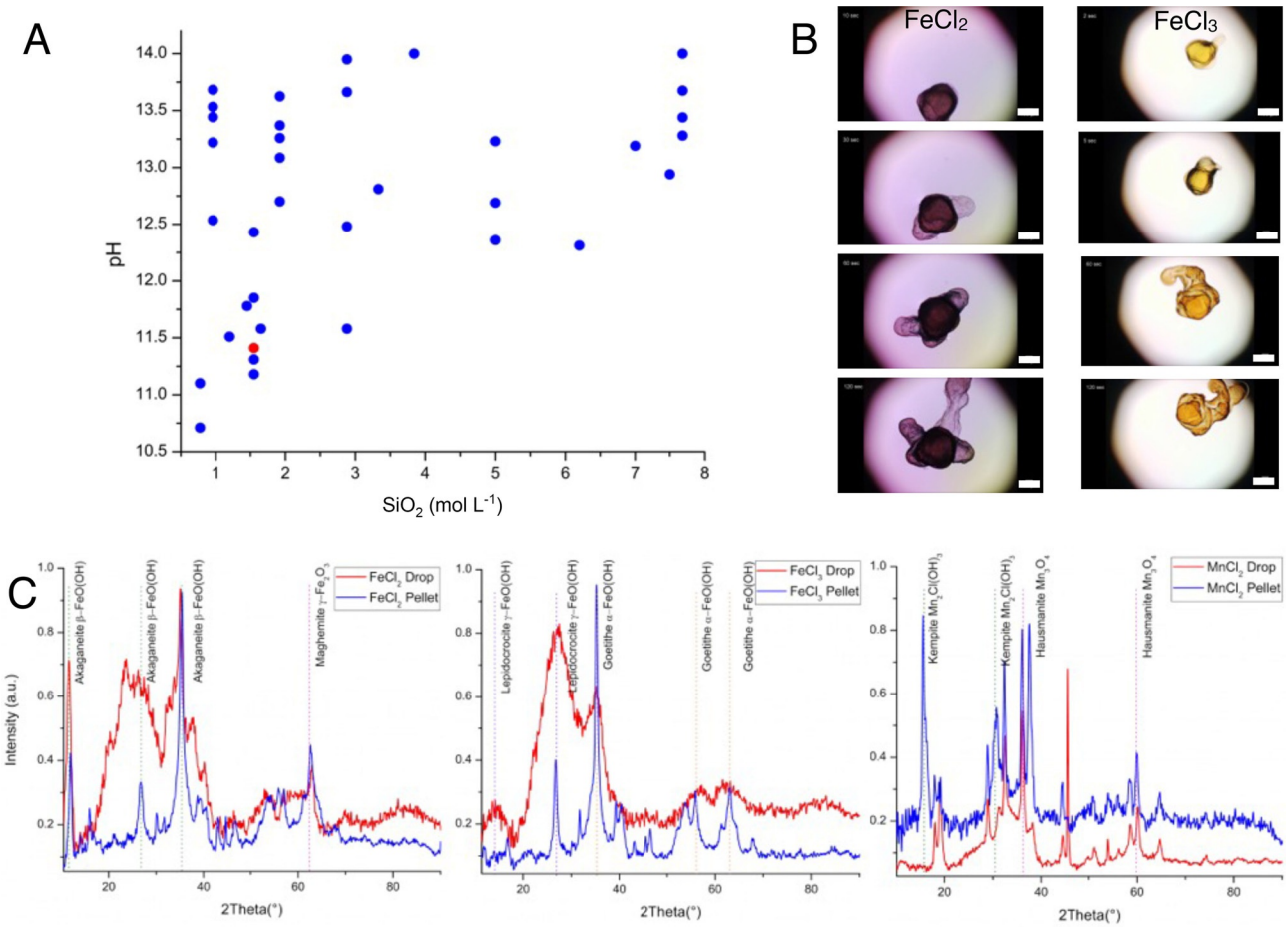

Figure 1. A) Screening of experimental conditions yielding metal–silica membranes. The red dot indicates the selected conditions for formamide condensation experiments. B) Frames of a time sequence of Fe^{2+} and Fe^{3+} membranes from Video S1 and Video S2 (in the Supporting Information, #1) recorded in the absence of formamide. Video S4 and Video S5 describing the Fe^{2+} and Fe^{3+} membranes growth in the presence of formamide are in the Supporting Information, #1. Scale bar: 250 microns. C) X-ray diffraction patterns of Fe^{2+}, Fe^{3+}, and Mn^{2+} membranes made with pellets and drops of the corresponding metals chlorides in the absence of formamide.

taining 10% (v/v) of NH_2CHO at room temperature. At the end of the reaction, the gel and the membrane were mechanically ground with a spatula in the presence of formamide (500 μL) to extract the products. Then, the residue was filtered and washed again with formamide (500 μL), and the solution distilled. The experiments were reproduced three times. The products were analyzed by gas chromatography-mass spectrometry (GC-MS) after formation of the corresponding trimethylsilyl ethers (TMS). GC-MS chromatograms are reported in the Supporting Information, #2. The analysis was limited to products $\geq 1\ ng\ mL^{-1}$, and the yield was calculated as milligrams of product per milliliter of starting NH_2CHO. The results of the experiments are shown in Figure 2 and Table 1. The reaction of formamide (10% v/v) with sodium silicate solution (pH 12) without inorganic membranes afforded only pyruvic acid **13**, lactic acid **14**, guanidine **22**, and urea **23**, in trace or very low amounts (micrograms).[20]

As a general trend, we observed the formation of a large panel of compounds of biological relevance, including nucleobases and their analogues, carboxylic acids, amino acids, and low molecular weight intermediates (Figure 2). The values and the peak abundances of products and the original *m/z* fragmentation spectra are in the Supporting Information, #3 and #4, respectively.

Nucleobases

The complete set of nucleobases of RNA [adenine (**2**), uracil (**3**), cytosine (**4**), and guanine (**6**)] and some nucleobase analogues, isocytosine (**5**), 4(3*H*)-pyrimidinone (**7**), and hypoxanthine (**12**), which are of relevance in the context of the origin of life and of chemiomimesis,[23–25] were obtained (Table 1). Purine (**11**), 6-hydroxy-2,4-diaminopyrimidine (**8**), 5-carboxy-2,4-diaminopyrimidine (**9**), and 3,5-diamino-1,2,4-triazole (**10**) were also detected in appreciable amounts. The mechanism of formation of nucleobases from NH_2CHO is reviewed,[26] with guanidine (**22**), urea (**23**), and diaminomalonitrile (**24**) being well-known key intermediates in the synthesis of both purine and pyrimidine derivatives.

$ZnCl_2$ and $MnCl_2$ provided only guanine **6**, and $CuCl_2$ only uracil **3**. However, $Fe_2(SO_4)_3{\cdot}9H_2O$, $MgSO_4$, and CuN_2O_6 afforded the complete panel of natural nucleobases **2**–**4** and **6**. As for

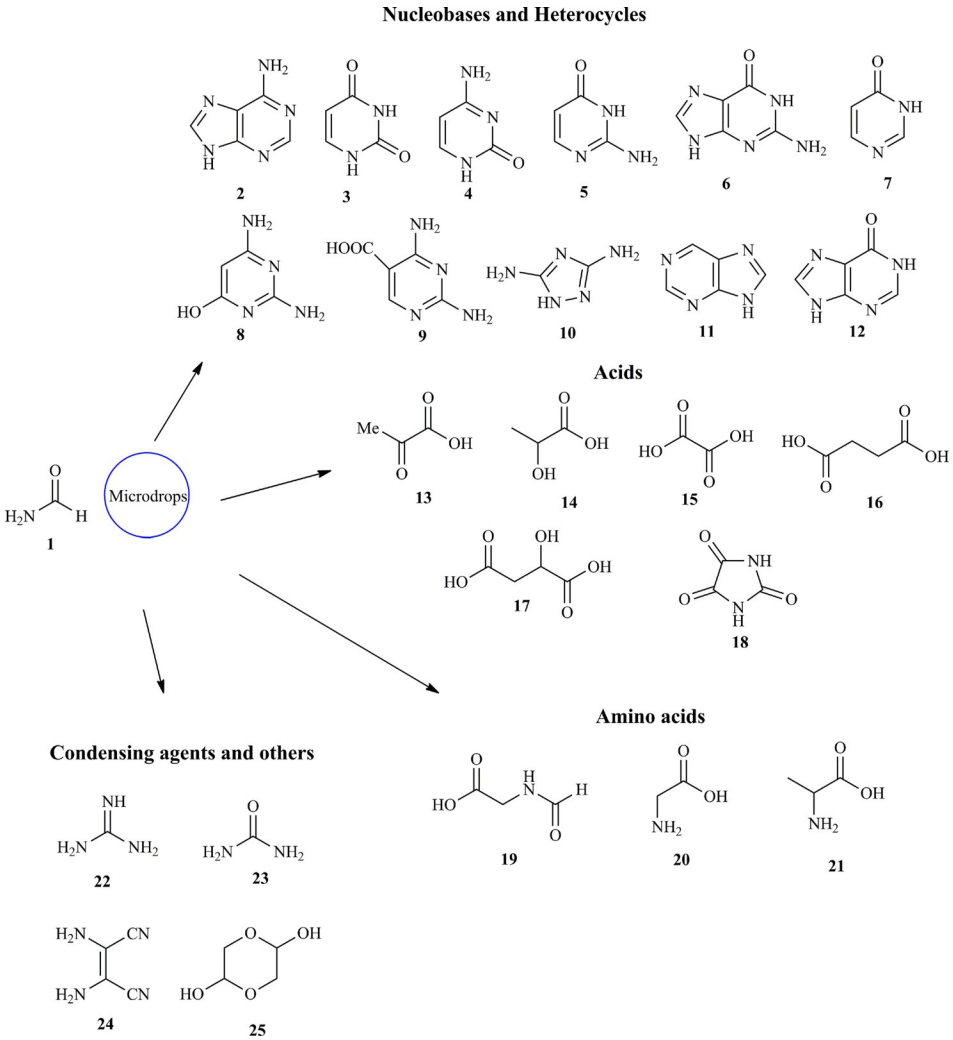

Figure 2. Schematic representation of products obtained during the thermal condensation of formamide and water in the presence of mineral vesicles. The products are classified on the basis of their biological role: nucleobases and heterocycles, acids, amino acids, and condensing agents.

Table 1. Products obtained by thermal condensation of NH_2CHO in the presence of active silica metal oxide/hydroxide membranes.[a]

Product[b,c]	$ZnCl_2$	$FeCl_2$	$CuCl_2$	$MnCl_2$	$Fe_2(SO_4)_3$	$MgSO_4$	$Cu(NO_3)_2$
adenine	–	–	–	–	1.20	0.62	0.43
(**2**)					(0.01)	(0.01)	(traces)
uracil	–	–	3.85	–	0.27	4.35	0.09
(**3**)			(3.8)		(0.22)	(0.23)	(–)
cytosine	–	traces	–	traces	1.69	4.9	0.5
(**4**)		(–)		(–)	(0.18)	(0.15)	(–)
isocytosine	0.06	traces	–	–	8.63	0.55	0.05
(**5**)	(–)	(–)			(0.11)	(–)	(–)
guanine	0.02	–	–	1.12	0.02	0.03	0.04
(**6**)							
4(3*H*)-pyrimidinone	traces	–	–	1.33	3.5	7.45	0.27
(**7**)	(–)			(0.3)	(traces)	(traces)	(0.05)
6(OH)-2,4-DAP	–	–	0.12	0.83	–	–	–
(**8**)				(0.06)			
2,4-DAP-5COOH	6.7×10^{-3}	–	–	3.65	0.45	3.4	3.08
(**9**)	(–)			(–)	(traces)	(traces)	(0.14)
triazole	0.23	–	0.05	–	0.39	1.13	–
(**10**)	(–)		(–)	(–)	(–)		
purine	4.65	0.01	0.02	–	0.38	0.05	traces
(**11**)	(–)	(–)	(–)		(–)	(–)	(–)
hypoxanthine	–	–	–	–	1.68	0.75	–
(**12**)						(–)	
pyruvic acid	3.5×10^{-4}	0.01	traces	2.60	0.08	0.91	0.37
(**13**)		(0.01)		(–)	(0.07)	(0.71)	(0.28)
lactic acid	0.14	0.81	2.85	–	1.65	–	0.01
(**14**)	(0.15)	(0.63)	(–)		(0.21)		(–)
oxalic acid	0.05	0.21	0.32	0.5	0.85	0.50	2.75
(**15**)	(2.8×10^{-3})	(0.18)	(0.10)	(–)	(0.38)	(0.12)	(–)
succinic acid	8.6×10^{-3}	–	1.15	0.31	0.23	0.95	1.65
(**16**)	(–)		(0.16)	(–)	(0.21)	(0.24)	(0.18)
oxaloacetic	–	2.3	3.05	1.19	0.16	0.22	0.25
(**17**)		(–)	(–)	(–)			(–)
parabanic	0.03	–	–	1.35	0.17	0.05	0.95
(**18**)	(–)			(–)	(–)	(–)	(0.9)
N-formylgly	–	–	–	traces	1.67	1.21	0.12
(**19**)				(–)	(9.0×10^{-3})	(–)	(–)
glycine	–	-	traces	-	0.62	0.68 (0.53)	0.04
(**20**)			(–)		(0.57)		(–)
alanine	0.07	traces	-	–	0.03	0.02	traces
(**21**)	(–)	(–)			(–)	(–)	(–)
guanidine	0.03	–	–	–	0.04	0.03	0.8
(**22**)	(5.2×10^{-3})				(–)	(–)	(0.67)
urea	7.4×10^{-3}	–	2.5	0.21	0.58	0.18	–
(**23**)	(2.0×10^{-3})		(2.6)	(5.0×10^{-3})	(0.02)	(–)	
DAMN	–	–	–	1.125	traces	traces	0.04
(**24**)				(–)	(–)	(–)	(–)
glycol aldehyde dimer	2.6×10^{-3}	–	0.02	traces	traces	traces	–
(**25**)	(–)		(–)	(–)	(–)	(–)	

[a] The yield is reported as amount (mg) of isolated products. The data are the mean values of three experiments with standard deviations of less than 0.1%. [b] Values in parentheses refer to results obtained in the presence of preformed metal silicate membranes under similar experimental conditions. [c] The reaction of formamide (10% v/v) with sodium silicate solution (pH 12) without inorganic membranes afforded only pyruvic acid **13**, lactic acid **14**, guanidine **22**, and urea **23**, in traces or in very low amount (micrograms).[20]

the order of reactivity, $MgSO_4$ afforded the highest total amount of nucleobases (9.9 mg), followed by $Fe_2(SO_4)_3{\cdot}9H_2O$ (3.18 mg) and $Cu(NO_3)_2$ (1.06 mg). Remarkably, the four nucleobases are here obtained in a one-pot reaction and in a synthetic set-up fed only by thermal energy. This observation is unprecedented.

Previous studies have reported the prebiotic synthesis of guanine[9,27,28] by using UV or proton irradiated solutions, but this is the first time the complete set of four RNA nucleobases are obtained under thermal conditions alone. According to data previously described,[7] adenine **2** and guanine **6** are produced from NH_2CHO by the same reaction pathway. This includes the initial formation of the HCN tetramer diaminomaleonitrile (DAMN), the cyclization to aminoimidazole carbonitrile (AICN), and the closure of the pyrimidine ring (by further addition of NH_2CHO and ammonia). The fact that different catalysts yield the same products hints at the robustness of formamide chemistry.

Carboxylic acids are key intermediates of numerous processes and metabolic cycles required in the cell for the production of energy and for the biosynthesis of primary and secondary metabolites. Mineral vesicles afforded six carboxylic acids including pyruvic acid (**13**), lactic acid (**14**), oxalic acid (**15**), succinic acid (**16**), oxaloacetic acid (**17**), and parabanic acid (**18**) (Figure 2, Table 1). In terms of biological relevance, oxalic acid and lactic acid are involved in the glyoxylate cycle,[29] in the Cori cycle, and in gluconeogenesis,[30] whereas pyruvic acid, succinic acid, and oxaloacetic acid are intermediates of the citric acid cycle [tricarboxylic acid cycle or Krebs cycle (KC)], one of the most ancient processes in cell metabolism. The KC is, in its reversed version, a prebiotic device for the production of energy and organics in the carbon-oxide-rich primitive atmosphere.[31] The formation of carboxylic acids **13**–**17** has been previously explained by the oligomerization of DAMN (actually detected in the reaction mixture), followed by hydrolysis and successive redox processes.[32] Parabanic acid **18** is a product of the degradation of both purine and pyrimidine nucleobases.[33,34] All salts were effective catalysts for the production of carboxylic acids. In addition to $CuCl_2$, $Fe_2(SO_4)_3{\cdot}9H_2O$ and $Cu(NO_3)_2$ were the best catalysts.

Amino acids

The formation of three amino acids—glycine (**20**), alanine (**21**), and *N*-formylglycine (**19**)—was observed. Amino acids are probably synthesized through a Strecker-like mechanism (Strecker-cyanohydrin), in accordance with the recent theoretical observations on the key role of NH_2CHO in the Miller–Urey synthesis of amino acids (**14**). *N*-Formylglycine **19** is produced from **20** by a NH_2CHO-based formylation process involving "in situ" generated carbodiimide (not isolated in this case), guanidine **22**, and urea **23**.[35] Amino acids were synthesized (with the sole exception of alanine) only in the presence of $Fe_2(SO_4)_3{\cdot}9H_2O$, $Cu(NO_3)_2$, and $MgSO_4$, with the iron salt being the most reactive catalyst.

These results show the higher reactivity of the silica metal oxyhydroxide membranes of the mineral vesicles when compared with the data previously obtained by using preformed metal silicate membranes prepared with classical silica garden experiments.[20] For an equal amount of salt, both the yield and the variety of synthesized products are enhanced: guanine, hypoxanthine, oxaloacetic acid, and alanine have been obtained by using only active mineral vesicles (Table 1). In classical chemical garden experiments, previously grown membranes were added to the acidic and alkaline solutions, mimicking the inner and outer solutions.[20] Different panels of products were observed for the experiments, with carboxylic acids prevailing in the experiment with tubular structures within the outside solutions, whereas nucleobases prevailed for the inside solutions. During the formation of the mineral vesicles, NH_2CHO experiences successively two different reaction environments, that is, the internal acidic metal-rich and the external alkaline silicate-rich solution, with the reaction products of the inner part of the membrane being released into the bulk of the solution upon the breaking of the membrane. Moreover, NH_2CHO condensation occurs during the formation of the membrane, thus benefiting from the ionic exchange and electric field processes.[18] However, the most important factor explaining the better yield of the active microdrops experiments is the lower crystallinity of the metal oxide/hydroxide phases found in microdrop-driven experiments with respect to silica gardens made with pellets (Figure 1C). Although the yield obtained with microdrops is notably high, it must be considered that they were obtained in the absence of irradiation. The irradiation of these experiments with protons or ultraviolet light is expected to enhance the yield and increase the number of biochemically relevant molecules. The study of the effect of UV radiation will be particularly interesting because iron/silica precipitates are supposed to screen it.[36]

As shown in Table 1, the best catalysts for the NH_2CHO condensation among the different salts tested are $Fe_2(SO_4)_3{\cdot}9H_2O$ and $MgSO_4$ (Table 1). Iron and magnesium are the two cations in the mineral composition of olivine, and they are also found in pyroxenes. Olivine and pyroxene are the main rock-forming minerals of the ultramafic and komaititic crust of the earliest Earth. The serpentinization reaction taking place when these minerals interact with water[15] is responsible for most of the compounds produced abiotically on the planet. Consequently, those geological sites where serpentinization is occurring are considered among the most likely niches for the transition from inorganic to organic geochemistry, and perhaps for the emergence of life. Along with Mn and Cu, the oxyhydroxides of these four metals account for the four nucleobases of the RNA and three amino acids obtained by condensation of NH_2CHO.

Conclusions

We conclude that the four nucleobases required for RNA synthesis, three amino acids (glycine, alanine, and *N*-formyl glycine), and six carboxylic acids can be synthesized from formamide in a single geochemical scenario at 80 °C, without irradiation. The condensation of formamide is catalyzed during the formation of silica oxyhydroxide membranes of iron, magnesium, manganese, and copper—common metals in the ultramafic and komaititic rocks of the earliest crust of the planet—as clearly highlighted by the comparison with the reaction performed in the absence of mineral vesicles. These membranes have been demonstrated to form within alkaline waters derived from the serpentinization reaction,[20] a common phenomenon on primitive Earth, and in Earth-like planets and moons. It is reasonable that the enhanced catalytic properties of the mineral vesicles obtained with microdrops with respect to silica gardens might be due their smaller size (and consequent higher surface area), and to the fact that they are actively formed during formamide condensation. Our results suggest that the conditions required for the synthesis of the molecular bricks from which life self-assembles, rather than being local and bizarre, appear to be universal and geologically conventional.

Experimental Section

Preparation of silica–metal oxide mineral vesicles with microdrops

The synthesis of mineral vesicles by using drops instead of solid pellets of the acidic salt has been investigated by a) pouring and b) injecting drops of saturated solutions of $FeCl_3$ [>97% Sigma–Aldrich, pH 0.68(3)], $FeCl_2$ (≥99% Sigma–Aldrich, pH 1.5), and $MnCl_2{\cdot}4H_2O$ [ACS reagent >98% Sigma–Aldrich, pH 2.06(5)] on and into sodium silicate solutions. Screening of the three main variables, namely silica concentration, pH of the silicate solution, and the volume of the iron solution drop (Figure 1), was performed. The pH values tested range from 10 to 14. The SiO_2 concentration ranges from 0.75 to 7.75 mol L^{-1}. The formation of membranes separating an inner metal-rich solution from the outer silica-rich solution depends on the concentration of silica and on pH (Figure 1). At high silica concentration and low pH, the gelling of the silica solution precludes the formation of the mineral membranes. As shown in Figure 1A, in all the other conditions tested (black dots) we observed the formation of membranes. The formation of silica metal oxide/hydroxide membranes was video-recorded by using a Nikon AZ10 microscope and a Nikon DSFi1 camera (Figure 1B). Videos S1–S6 describing the growth of membranes in the presence or in the absence of formamide, in the case of different salts, are in the Supporting Information, #1. The pH was measured with a pH electrode (Mettler Toledo InLab Expert Pro_15M, tip diameter: 3 mm), and a laboratory pH meter (Eutech Instruments pH 510). The precipitating membranes were analyzed by X-ray powder diffraction in the absence of formamide. They were first harvested and rinsed thoroughly with water and ethanol. They were dried and ground to fine powder. Powder diffraction measurements were performed with a PANalytical X'Pert diffractometer operating at a wavelength of 1.54 Å ($Cu_{K\alpha}$ radiation). The measured 2θ range was chosen as 10–90° in steps of 0.02°. The integration time per step was set to 22 s. Assignment and identification of detected reflexes to crystalline matter was accomplished by using the reference library of the X'Pert HighScore Plus-PDF2. The occurring phases of $FeCl_3$ include lepidocrocite γ-FeO(OH) and goethite α-FeO(OH). In the case of $FeCl_2$, the phases identified were akagaenite β-FeO(OH) and maghemite γ-Fe_2O_3. For $MnCl_2$ membranes, the identified phases were hausmannite Mn_3O_4 and kempite $Mn_2Cl(OH)_3$. The crystallinity of the mineral vesicles formed by microdrops is lower compared with the ones made with solid pellets, as seen from X-ray diffraction study (Figure 1C).

Thermal condensation of formamide

Formamide (Fluka, >99%) was used without further purification. Fresh commercial sodium silicate solution (Sigma–Aldrich, reagent grade, containing about 13.8 wt% Na and 12.5 wt% Si) was used as the silica source after 1:4 (v/v) dilution with Millipore water. Typically, 1.8 mL of this sodium silicate solution was mixed with 200 μL of formamide. The presence of formamide did not change the pH of the alkaline silicate solution but it accelerated the gelling process. Before gelling, 10 microdrops (5 μL each) of the saturated solution of the metal salts were added by pouring. We tested $ZnCl_2$, $FeCl_2{\cdot}4H_2O$, $CuCl_2{\cdot}2H_2O$, $MnCl_2$, $Fe_2(SO_4)_3{\cdot}9H_2O$, CuN_2O_6, and $MgSO_4$. Microdrops were observed to expand immediately and the reaction mixture was heated at 80 °C for 24 h. After some hours (4–8 h, depending on the nature of the salt), a low-density gel appeared and the reaction products were recovered by the following procedure: a) the gel and the membrane were broken off with a spatula with addition of formamide (500 μL); b) filtration of the in-

Table 2. Mass-to-charge ratio (*m/z*) value and the abundance of mass spectra peaks of compounds (**2**–**25**).

Products[a]	*m/z* (%)
adenine[c] (**2**)	279 (27) [*M*], 264 (100) [*M*−CH_3], 249 (1) [*M*−$(CH_3)_2$], 192 (17)
uracil[c] (**3**)	256 (35) [*M*], 241 (100) [*M*−CH_3], 225 (15) [*M*−CH_3−CH_4], 182 (7) [*M*−$Si(CH_3)_3$−H_2], 142 (70), 113 (55)
cytosine[c] (**4**)	255 (49) [*M*], 254 (100) [*M*−H], 240 (72) [*M*−CH_3], 182 (5) [*M*−$HSi(CH_3)_3$]
isocytosine[d] (**5**)	327 (18) [*M*], 312 (100) [*M*−CH_3], 282 (9) [*M*−$(CH_3)_3$], 255 (6) [*M*−$Si(CH_3)_3$], 240 (7) [*M*−$HSi(CH_3)_3$−CH_3], 183 (2) [*M*−2×$Si(CH_3)_3$]
guanine (**6**)	367 (100) [*M*], 352 [*M*−CH_3], 294 [*M*−$HSi(CH_3)_3$]
4(3*H*)-pyrimidinone[b] (**7**)	168 (25) [*M*], 153 (100) [*M*−CH_3], 123 (5) [*M*−$(CH_3)_3$], 99 (100)
6-(OH)-2,4-DAP[c] (**8**)	270 (35) [*M*], 255 (100) [*M*−CH_3]
2,4-DAP-5-COOH[d] (**9**)	370 (11) [*M*], 355 (100) [*M*−CH_3]
3,5-(NH_2)-1,2,4 triazole[c] (**10**)	243 (65) [*M*], 230 (100) [*M*−CH_3]
purine[b] (**11**)	192 (100) [*M*], 177 (100) [*M*−CH_3]
hypoxanthine (**12**)	280 (30) [*M*−$Si(CH_3)_3$] 265 (100) [*M*−$Si(CH_3)_3$−CH_3]
pyruvic acid[c] (**13**)	160 (10) [*M*], 145 (7) [*M*−CH_3], 88 (14) [*M*−$Si(CH_3)_3$], 71 (12) [*M*−$Si(CH_3)_3$−OH], 43 (100) [*M*−$HSi(CH_3)_3$−CO_2]
lactic acid[c] (**14**)	219 (6) [*M*−CH_3], 190 (14) [*M*−CO_2], 147 (71) [*M*−$Si(CH_3)_3$−CH_3], 133 (7), 117 (76) [*M*−$Si(CH_3)_3$−$(CH_3)_3$]
oxalic acid[c] (**15**)	219 (3) [*M*−CH_3], 189 (5) [*M*−$(CH_3)_3$], 147 (78) [*M*−$Si(CH_3)_3$−CH_3], 117 (1) [*M*−$Si(CH_3)_3$−3×CH_3], 73 (100)
succinic acid[c] (**16**)	247 (16) [*M*−CH_3], 173 (5) [*M*−$HOSi(CH_3)_3$], 147 (100), 73 (80)
oxaloacetic acid (**17**)	346 (10) [*M*], 333 (100) [*M*−CH_3]
parabanic acid[c] (**18**)	258 (15) [*M*], 243 (35) [*M*−CH_3], 215 [*M*−2×CH_3], 100 (100), 73 (23)
N-formylglycine[b] (**19**)	160 (38) [*M*−CH_3], 147 (5) [*M*−CO], 131 (22) [*M*−$CONH_2$], 102 (11) [*M*−$Si(CH_3)_3$], 73 (100)
glycine[b] (**20**)	147 (11) [*M*], 132 (28) [*M*−CH_3], 88 (9), 73 (100)
alanine[c] (**21**)	218 (4) [*M*−CH_3], 190 (6), 147 (13), 116 (100) [*M*−$HOSi(CH_3)_3$−CO], 73 (60)
guanidine[c] (**22**)	188 (11) [*M*−CH_3], 173 (10) [*M*−2×CH_3], 171 (100), 73 (33)
urea[c] (**23**)	204 (7) [*M*], 189 (73) [*M*−CH_3], 147 (100), 73 (35)
DAMN[c] (**24**)	252 (5) [*M*], 153 (18) [*M*−$Si(CH_3)_3$−HCN], 138 (3) [*M*−$NHSi(CH_3)_3$−HCN], 73 (100) [$Si(CH_3)_3$]
glycol aldehyde dimer[c] (**25**)	264 (4) [*M*], 191 (95) [*M*−$Si(CH_3)_3$]

[a] Mass spectroscopy was performed by using a GC-MS. Samples were analyzed after treatment with *N*,*N*-bis-trimethylsilyl trifluoroacetamide and pyridine. The peak abundance is reported in parentheses. [b] Product analyzed as the monosilyl derivative. [c] Product analyzed as the bis-silyl derivative. [d] Product analyzed as the tris-silyl derivative.

organic material and the gel by using a Büchner funnel (washing with (500 μL) of formamide and recovering the liquid phase); c) high vacuum distillation of the liquid phase to obtain a crude (SiO_2 + reaction products); d) direct analysis of the reaction products by silylation of the crude. The crude was analyzed by gas chromatography associated with mass spectrometry (GC-MS) after treatment with *N*,*N*-bis-trimethylsilyl trifluoroacetamide in pyridine (620 μL) at 60 °C for 4 h in the presence of oleic acid as the internal standard (0.2 mg). Mass spectrometry was performed through the following program: injection temperature 280 °C, detector temperature 280 °C, gradient 100 °C for 2 min, and 10 °C min^{-1} for 60 min. To identify the structure of the products, two strategies were followed. First, the spectra were compared with commercially available electron mass spectra libraries such as NIST (Fison, Manchester, UK). Second, GC-MS analysis was repeated with standard compounds. All products have been recognized with a similarity index (SI) greater than 98% compared with that of the reference standards. The analysis was limited to products of ≥ 1 ng mL^{-1}, and the yield was calculated as milligrams of isolated products. Mass-to-charge ratio (*m*/*z*) values and the abundance of mass spectra peaks of compounds **2**–**25** are reported in Table 2.

Acknowledgments

We acknowledge funding from the European Research Council under the European Union's Seventh Framework Programme (FP7/2007–2013)/European Research Council grant agreement no. 340863 (Prometheus). Ministerio de Economia *y* Competitividad is acknowledge for Project CGL2016-78971-P, AEI/FEDER. MIUR Ministero dell'Istruzione, dell'Università della Ricerca and Scuola Normale Superiore (Pisa, Italy), project PRIN 2015 STARS in the CAOS: Simulation Tools for Astrochemical Reactivity and Spectroscopy in the Cyberinfrastructure for Astrochemical Organic Species, cod. 2015F59J3R, is acknowledged. This work was supported by COST Action TD 1308. M.I.P.V. acknowledges financial support from CONACyT (CVU 557501/300081) and VIEP-BUAP.

Conflict of interest

The authors declare no conflict of interest.

Keywords: biomolecules and condensing agents · catalysis · formamide · prebiotic chemistry · silica microdrops

[1] A. G. Cairns-Smith, *Genetic Takeover and the Mineral Origins of Life*, Cambridge University Press, Cambridge, **1982**, p. 278.
[2] V. Goldschmidt, *New Biol.* **1952**, *12*, 97 – 105.
[3] J. Bernal, *The Origin of Life*, World Publishing Company, Cleveland, **1967**.
[4] L. E. Orgel, *Crit. Rev. Biochem. Mol. Biol.* **2004**, *39*, 99 – 123.
[5] M. Ferus, F. Pietrucci, A. M. Saitta, A. Knížeka, P. Kubelíka, O. Ivaneka, V. Shestivska, S. Civiš, *Proc. Natl. Acad. Sci. USA* **2017**, *114*, 4306 – 4311.
[6] a) J. Oró, S. Kamat, *Nature* **1961**, *190*, 442 – 443; b) B. H. Patel, C. Percivalle, D. J. Ritson, C. D. Duffy, J. D. Sutherland, *Nat. Chem.* **2015**, *7*, 301 – 307.
[7] M. Ferus, *Proc. Natl. Acad. Sci. USA* **2015**, *112*, 657 – 662.
[8] E. Carota, G. Botta, L. Rotelli, E. Di Mauro, R. Saladino, *Curr. Org. Chem.* **2015**, *19*, 1963 – 1979.
[9] R. Saladino, E. Carota, G. Botta, M. Kapralov, G. N. Timoshenko, A. Y. Rozanov, E. Krasavin, E. Di Mauro, *Proc. Natl. Acad. Sci. USA* **2015**, *112*, E2746 – E2755.
[10] A. López-Sepulcre, A. A. Jaber, E. Mendoza, B. Lefloch, C. Ceccarelli, C. Vastel, R. Bachiller, J. Cernicharo, C. Codella, C. Kahane, M. Kama, M. Tafalla, *Mon. Not. R. Astron. Soc.* **2015**, *449*, 2438 – 2458.
[11] G. R. Adande, N. J. Woolf, L. M. Ziurys, *Astrobiology* **2013**, *13*, 439 – 453.
[12] N. Biver, D. Bockelée-Morvan, V. Debout, J. Crovisier, J. Boissier, D. C. Lis, N. Dello Russo, R. Moreno, P. Colom, G. Paubert, R. Vervack, H. A. Weaver, *Astron. Astrophys.* **2014**, *566*, L5.
[13] D. Bockelée-Morvan, D. C. Lis, J. E. Wink, D. Despois, J. Crovisier, R. Bachiller, D. J. Benford, N. Biver, P. Colom, J. K. Davies, E. Gerard, B. Germain, M. Houde, D. Mehringer, R. Moreno, G. Paubert, T. G. Phillips, H. Rauer, *Astron. Astrophys.* **2000**, *353*, 1101 – 1114.
[14] A. M. Saitta, F. Saija, *Proc. Natl. Acad. Sci. USA* **2014**, *111*, 13768 – 13773.
[15] N. H. Sleep, A. Meibom, T. Fridriksson, R. G. Coleman, D. K. Bird, *Proc. Natl. Acad. Sci. USA* **2004**, *101*, 12818 – 12823.
[16] A. Neubeck, N. T. Duc, D. Bastviken, P. Crill, N. G. Holm, *Geochem. Trans.* **2011**, *12*, 6.
[17] J. M. García-Ruiz, E. Nakouzi, E. Kotopoulou, L. Tamborrino, O. Steinbock, *Sci. Adv.* **2017**, *3*, e1602285.
[18] F. Glaab, M. Kellermeier, W. Kunz, E. Morallon, J. M. García-Ruiz, *Angew. Chem.* **2012**, *124*, 4393 – 4397.
[19] L. M. Barge, Y. Abedian, M. J. Russell, I. J. Doloboff, J. H. E. Cartwright, R. D. Kidd, I. Kanik, *Angew. Chem. Int. Ed.* **2015**, *54*, 8184 – 8187; *Angew. Chem.* **2015**, *127*, 8302 – 8305.
[20] R. Saladino, G. Botta, B. M. Bizzarri, E. Di Mauro, J. M. Garcia Ruiz, *Biochemistry* **2016**, *55*, 2806 – 2811.
[21] F. Glaab, J. Rieder, R. Klein, D. Choquesillo-Lazarte, E. Melero-Garcia, J. M. García-Ruiz, W. Kunz, M. Kellermeier, *ChemPhysChem* **2017**, *18*, 338 – 345.
[22] M. Kellermeier, F. Glaab, E. Melero-García, J. M. García-Ruiz, *Meth. Enzymol.* **2013**, *532*, 225 – 256.
[23] R. Saladino, G. Botta, S. Pino, G. Costanzo, E. Di Mauro, *Front. Biosci.* **2013**, *18*, 1275 – 1289.
[24] H. D. Bean, Y. Sheng, J. P. Collins, F. A. L. Anet, J. Leszczynski, N. V. Hud, *J. Am. Chem. Soc.* **2007**, *129*, 9556 – 9557.
[25] I. Hirao, M. Kimoto, R. Yamashige, *Acc. Chem. Res.* **2012**, *45*, 2055 – 2065.
[26] M. Ferus, S. Civiš, A. Mládek, J. Šponer, L. Juha, J. E. Šponer, *J. Am. Chem. Soc.* **2012**, *134*, 20788 – 20796.
[27] S. Senanayake, H. Idriss, *Proc. Natl. Acad. Sci. USA* **2006**, *103*, 1194 – 1198.
[28] H. L. Barks, R. Buckley, G. A. Grieves, E. Di Mauro, N. V. Hud, T. M. Orlando, *ChemBioChem* **2010**, *11*, 1240 – 1243.
[29] K. Storrey, *Functional Metabolism: Regulation and Adaptation*, Wiley, Hoboken, **2004**.
[30] W. D. McArdle, F. I. Katch, V. L. Katch, *Exercise Physiology: Mutrition, Energy, and Human Performance*, Lippincott Williams & Wilkins, Philadelphia, **2010**.
[31] E. Smith, H. J. Morowitz, *Proc. Natl. Acad. Sci. USA* **2004**, *101*, 13168 – 13173.
[32] A. Eschenmoser, *Chem. Biodiversity* **2007**, *4*, 554 – 573.
[33] N. Jena, P. Mishra, *Free Radical Biol. Med.* **2012**, *53*, 81 – 94.
[34] C. Menor-Salván, M. R. Marín-Yaseli, *Chem. Eur. J.* **2013**, *19*, 6488 – 6497.
[35] R. Saladino, G. Botta, S. Pino, G. Costanzo, E. Di Mauro, *Chem. Soc. Rev.* **2012**, *41*, 5526 – 5565.
[36] V. Phoenix, K. Konhauser, D. Adams, S. Bottrell, *Geology* **2001**, *29*, 823 – 826.

Manuscript received: December 29, 2017
Accepted manuscript online: March 30, 2018
Version of record online: May 14, 2018

